Nonlinear Relations to Final Semi-Major Axis in Continuous Orbital Transfers

A.D.C. Jesus[1†], M.L.O. Souza[2] and A.F.B.A. Prado[2]

[1]*Departamento de Física, Universidade Estadual de Feira de Santana (UEFS),*
Caixa Postal 252-294, BR116-Norte, Km 3, 44.031-460, Feira de Santana, BA, Brazil
[2]*Instituto Nacional de Pesquisas Espaciais (INPE), Avenida dos Astronautas 1758,*
Caixa Postal 515, 12227-010, São José dos Campos, SP, Brazil

Abstract: We studied nonimpulsive orbital transfers under thrust errors through algebraic analysis method. We analyzed the relationship among final semi-major axis and mean deviations in the thrust vector. The nonlinear (near parabolic) relations were found, confirming the Monte-Carlo simulations realized in the numerical phase this investigation. These results suggest and partially characterize the progressive deformation of the final semi-major axis along the propulsive arc, turning 3sigma ellipsoids into banana shaped volumes curved to the center of attraction (we call them "bananoids") due to the loss of optimality of the actual (with errors) trajectories with respect to the nominal (no errors) trajectory.

Keywords: *Orbits; transfer; nonimpulsive; thrust errors; algebraic analysis.*

Mathematics Subject Classification (2000): 70M20, 65C05, 62L70.

1 Introduction

According to Marec [1], the orbital transfer of a space vehicle under the gravitational attraction of a celestial body is one of the classical and important problems of Astronautics. Since the early decades of XX century, many researchers dedicated much attention and interest to this problem. Ideally, we can say that, to transfer a space vehicle from one orbit to other consists of changing its initial state, defined by its position, velocity and mass $(\vec{r_0}, \vec{v_0}, m_0)$ in a certain initial instant t_0, to another state, defined by its respective state variables $(\vec{r_f}, \vec{v_f}, m_f)$ in a final instant $t_f > t_0$. When the transfer is done aiming to minimize the fuel spent, we define the "Fundamental Problem of Astronautics", that is,

---

to transfer a vehicle, changing its initial state to a final state with the smallest possible fuel spent $(m_0 - m_f)$. According to Jesus [2], orbital transfers are done to meet some objectives under some restrictions that can be put into the problem to obtain the best possible performance for a particular mission. Examples of objectives are minimum fuel consumption, minimum transfer time, maximum final velocity, etc. Examples of restrictions are rendezvous of two vehicles, the transfer between two given points in a fixed time (Lambert problem), etc. In this way, we can consider that the orbital transfer problem, despite basic in nature, present challenges with respect to its general characteristics since diverse natural, modeling, economic, operational limitations need to be considered in its formulation. So, to find the desired optimal solutions, different problem formulations and optimization criteria can be used to best approximate it to the actual case. The actuator models are normally used in the orbital transfer or correction problems. The infinite propulsion, where the source is modeled as being capable of applying a large magnitude but small duration force (with respect to the orbital period) is the most used, but the non-impulsive hypothesis (finite propulsion) is also found in the literature under many different constraints. The applications of these maneuvers include: small orbital corrections of an Earth artificial satellite, to put a satellite in geostationary orbit, the rendezvous or intercept missions, the long interplanetary travels (like "Voyager" and "Pioneer" missions), the transportation and assembly of the International Space Station. In Brazil, they include: to put and to keep in orbit the Remote Sensing Satellites 1,2 and China-Brazil Earth Resources Satellites 1,2.

Most space missions need orbit transfers to reach their goals. These orbits are reached sequentially through transfers between them, by changing at least one component of the vehicle velocity or position vectors, that is, at least one of corresponding Keplerian elements by firing thrusts, apogee motors, or other force sources. The actual thrust vector has errors in magnitude and/or in direction with respect to the ideal thrust vector.

The magnitude errors are caused by many and unpredictable reasons as: limitations in the manufacturing process (mechanical imprecision due to mechanical and chemical machining, tolerances in the components, etc.) in the loading process (tolerances in the physical and chemical characteristics of the used substances, etc.), in the thrust operation (pulsed, blow-down, under the actual conditions, etc.). They can be modeled as: 1) a constant but random deviation ("random bias") with respect to the ideal magnitude, resulting in a constant actual mean magnitude with a certain probability density function (uniform in the worst case, Gaussian in the best case); and/or 2) random fluctuations around this actual mean magnitude with little or no correlation in time ("pink or white noise") and with a certain probability density function (uniform in the worst case, Gaussian in the best case).

The direction errors of misalignment's errors with respect to its nominal action line are caused by many and unpredictable reasons as: linear and angular displacements during the vehicle assembly and particularly, during the thrusts assembly; displacements of the center of mass during the injection in orbit/trajectory, and during the vehicle operation, due to movable parts as solar panels, antennas, booms, pendulums, etc., or due to fuel consumption, specially during their firing; many and asymmetric thrusts firing at the same time, dead zones existing in all attitude controls used during the firing; partial deviation of some jet plumes by the vehicle structure (plume impingement); etc. They can be modeled like the magnitude errors. These are the magnitude and direction errors models used in the work of Jesus [2].

So, most space missions need trajectory/orbit transfers and they have linear and/or angular misalignments that displace the vehicle with respect its nominal directions. The mathematical treatment for these deviations can be done under many approaches (deterministic, probabilistic, minimax, etc.)

In the deterministic approach: we highlight Schwende and Strobl [3], Tandon [4], Rodrigues [5], Santos-Paulo [6], Rocco [7] and Schultz [8], among others.

In the probabilistic approach Porcelli and Vogel [9] presented an algorithm for the determination of the orbit insertion errors in biimpulsive noncoplanar orbital transfers (perigee and apogee), using the covariance matrices of the sources of errors. Adams and Melton [10] extended such algorithm to ascent transfers under a finite thrust, modeled as a sequence of impulsive burns. They developed an algorithm to compute the propagation of the navigation and direction errors among the nominal trajectory, with finite perigee burns. Rao [11] built a semi-analytic theory to extend covariance analysis to long-term errors on elliptical orbits. Howell and Gordon [12] also applied covariance analysis to the orbit determination errors and they develop a station-keeping strategy of Sun-Earth L1 libration point orbits. Junkins, *et al.* [13] and Junkins [14] discussed the precision of the error covariance matrix method through nonlinear transformations of coordinates. He also found a progressive deformation of the initial ellipsoid of trajectory distribution (due to Gaussian initial condition errors), that was not anticipated by the covariance analysis of linearized models with zero mean errors. Its main results also characterize how close or how far are Monte-Carlo analysis and covariance analysis for those examples. Carlton-Wippern [15] proposed differential equations in polar coordinates for the growth of the mean position errors of satellites (due to errors in the initial conditions or in the drag), by using an approximation of Langevin's equation and a first order perturbation theory. Alfriend [16] studied the effects of drag uncertainty via covariance analysis.

In the minimax approach: see Russian authors, mainly.

However, all these analyses are approximated. This motivated an exhaustive numerical (see [17, 18]) but exact analysis (by Monte-Carlo), and a partial algebraic analysis done by Jesus [2]. In this work we present the first part of the algebraic analysis of nonimpulsive orbital transfers under thrust errors. The results were obtained for two transfers: the first, a low thrust transfer between high coplanar orbits (we call it "theoretical transfer"), used by Biggs [19, 20] and Prado [21]; the second, a high thrust transfer between middle noncoplanar orbits (the first transfer of the EUTELSAT II-F2 satellite, we call it "practical transfer") implemented by Kuga, *et al.* [22]. The simulations were done for both transfers with minimum fuel consumption. The "pitch" and "yaw" angles were taken as control variables such that the overall minimum fuel consumption defines each burn of the thrusts. The errors sources that we considered were the magnitude errors, the "pitch" and "yaw" direction errors of the thrust vector, as causes of the deviations found in the several Keplerian elements of the transfer trajectory. These errors sources (random-bias and white-noise errors) introduced in the orbital transfer dynamics produce effects in the final orbit Keplerian elements in the final instant.

In this work we present an algebraic analysis of the effects of these errors on the mean of the deviations of the Keplerian elements of the final orbit with respect to the reference orbit (final orbit without errors in the thrust vector) for both transfers. The approach that we used in this work for the treatment of the errors was the probabilistic one, assuming these as having zero mean Gaussian probability density function or having zero mean Uniform probability density function.
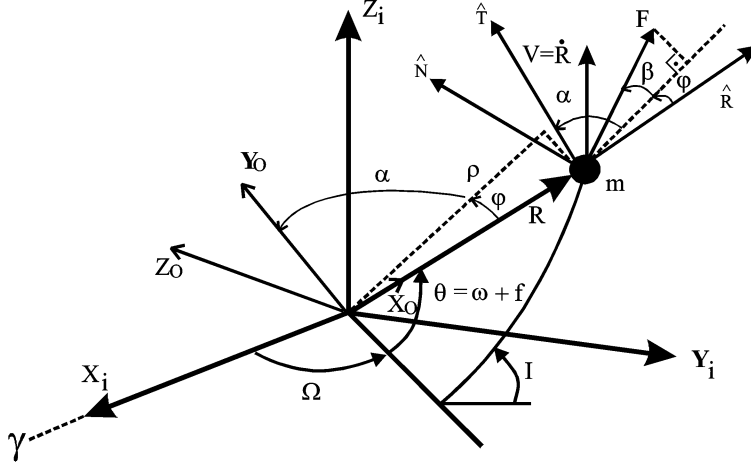
Figure 2.1.   Reference systems used in this work.

2 Mathematical Formulation and Coordinates Systems

The orbital transfer problem studied can be formulated in the following way:

1) Globally minimize the performance index: $J = m(t_0) - m(t_f)$;
2) With respect to $\alpha \colon [t_0, t_f] \to R$ ("pitch" angle) and $\beta \colon [t_0, t_f] \to R$ ("yaw" angle) with $\alpha, \beta \in C^{-1}$ in $[t_0, t_f]$;
3) Subject to the dynamics in inertial coordinates X_i, Y_i, Z_i of Figure 2.1: $\vee t \in [t_0, t_f]$;

$$m(t) \frac{d^2 X}{dt^2} = -\mu m(t) \frac{X}{R^3} + F_x, \tag{1}$$

$$m(t) \frac{d^2 Y}{dt^2} = -\mu m(t) \frac{Y}{R^3} + F_y, \tag{2}$$

$$m(t) \frac{d^2 Z}{dt^2} = -\mu m(t) \frac{Z}{R^3} + F_z, \tag{3}$$

$$\begin{aligned} F_x = F\big[&\cos\beta \sin\alpha(\cos\Omega \cos\theta - \sin\Omega \cos I \sin\theta) + \sin\beta \sin\Omega \sin I \\ &- \cos\beta \cos\alpha(\cos\Omega \sin\theta + \sin\Omega \cos I \cos\theta)\big] \end{aligned} \tag{4}$$

$$\begin{aligned} F_y = F\big[&\cos\beta \sin\alpha(\sin\Omega \cos\theta + \cos\Omega \cos I \sin\theta) - \sin\beta \cos\Omega \sin I \\ &- \cos\beta \cos\alpha(\sin\Omega \sin\theta - \cos\Omega \cos I \cos\theta)\big], \end{aligned} \tag{5}$$

$$F_z = F(\cos\beta \sin\alpha \sin I \sin\theta + \cos\beta \cos\alpha \sin I \cos\theta + \sin\beta \cos I), \tag{6}$$

$$m(t) = m(t_0) + \dot{m}(t - t_0) \tag{7}$$

with $\dot{m} < 0$

$$F \cong |\dot{m}|c. \tag{8}$$

Or in orbital coordinates (radial R, transverse T, and binormal N) of Figure 2.1:

$$m(t)a_R(t) = F\cos\beta(t)\sin\alpha(t) - \frac{\mu m(t)}{R^2(t)}, \tag{9}$$

$$m(t)a_T(t) = F\cos\beta(t)\cos\alpha(t), \tag{10}$$

$$m(t)a_N(t) = F\sin\beta(t), \tag{11}$$

$$a_R(t) = \dot{V}_R - \frac{V_T^2}{R} - \frac{V_N^2}{R}, \tag{12}$$

$$a_T(t) = \dot{V}_T + \frac{V_R V_T}{R} - V_N \dot{I}\cos\theta - V_N\dot{\Omega}\sin I\sin\theta, \tag{13}$$

$$a_N(t) = \dot{V}_N + \frac{V_R V_N}{R} + V_T\dot{I}\cos\theta + V_T\dot{\Omega}\sin I\sin\theta, \tag{14}$$

$$V_R = \dot{R}, \tag{15}$$

$$V_T = R(\dot{\Omega}\cos I + \dot{\theta}), \tag{16}$$

$$V_N = R(-\dot{\Omega}\sin I\cos\theta + \dot{I}\sin\theta), \tag{17}$$

$$\theta = \omega + f; \tag{18}$$

4) Given the initial and final orbits, and the parameters of the problem $(m(t_0), c, \dots)$. These equations were obtained by: 1) writing in coordinates of the dexterous rectangular reference system with inertial directions $0X_iY_iZ_i$ the Newton's laws for the motion of a satellite S with mass m, with respect to this reference system, centered in the Earth's center of mass 0 with X_i axis toward the Vernal point, X_iY_i plane coincident with Earth's Equator, and Z_i axis toward the Polar Star approximately; 2) rewriting them in coordinates of the dexterous rectangular reference system with radial, transverse, binormal directions $SRTN$, centered in the satellite center of mass S; helped by 3) a parallel system with $0X_0Y_0Z_0$ directions, centered in the Earth's center of mass 0, X_0 axis toward the satellite S, X_0Y_0 plane coincident with the plane established by the position $\vec{R}$ and velocity $\vec{V}$ vectors of the satellite, and Z_0 axis perpendicular to this plane; and helped by 4) the instantaneous Keplerian coordinates $(\Omega, I, \omega, f, a, e)$. These equations were later rewritten and simulated by using 5) 9 state variables, defined and used by Biggs [19, 20] and Prado [21], as functions of an independent variable s shown in Figure 2.2.

The non-ideal thrust vector, with magnitude and direction errors, is given by:

$$\vec{F_E} = \vec{F} + \Delta\vec{F}, \tag{19}$$

$$\vec{F_E} = \vec{F_R} + \vec{F_T} + \vec{F_N}, \tag{20}$$

$$|\vec{F_E}| = F_E, \quad |\vec{F}| = F, \tag{21}$$

$$F_R = (F + \Delta F)\cos(\beta + \Delta\beta)\sin(\alpha + \Delta\alpha), \tag{22}$$

$$F_T = (F + \Delta F)\cos(\beta + \Delta\beta)\cos(\alpha + \Delta\alpha), \tag{23}$$

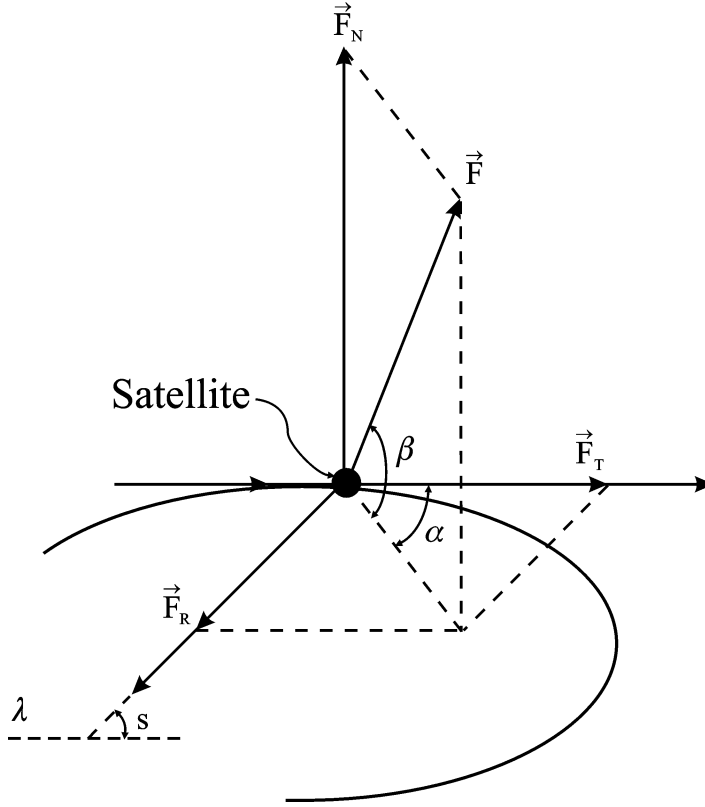$$F_N = (F + \Delta F)\sin(\beta + \Delta\beta), \tag{24}$$

Figure 2.2. Thrust vector applied to the satellite and the s variable.

where: $\vec{F}$, $\vec{F_E}$ and $\Delta\vec{F}$ are: the thrust vector without errors, the thrust vector with errors, and the error in the thrust vector, respectively; $\Delta\alpha$ and $\Delta\beta$ are the errors in the "pitch" and in the "yaw" angles, respectively; F_R, F_T and F_N are the components of the thrust vector with errors $\vec{F_E}$ in the radial, transverse and normal directions, respectively. In this way, for each implementation of the orbital transfer arc, values of α and β are chosen, whose errors are inside the range, that produce the direction for the overall minimum fuel consumption.

3 Transfers with Errors in the Thrust Vector: Algebraic Analysis

We start our algebraic analysis by planar $(\alpha \neq 0)$ and $(\beta = 0)$ transfer maneuvers. We also choose F and m constants. Under these hypotheses, Equations $(9)-(14)$ become:

$$F_t = m\dot{v}_t(t) = F\cos(\alpha(t)) - mv_r(t)\dot{f}(t), \tag{25}$$

$$F_r = m\dot{v}_r(t) = F\sin(\alpha(t)) + mv_t(t)\dot{f}(t) - \frac{\mu m(t)}{r^2(t)}, \tag{26}$$

$$\dot{f}(t) = \frac{v_t(t)}{r(t)}, \tag{27}$$

$$\dot{r}(t) = v_r(t), \tag{28}$$

with, F_t and F_r the transverse and radial components of the thrust vector, respectively; $\dot{v}_t(t)$, $\dot{v}_r(t)$ the transverse and radial components of the accelerations, respectively; $v_t(t)$, $v_r(t)$ the transverse and radial components of the velocities, respectively; $\dot{f}(t)$ the angular velocity; $r(t)$ the vector position between satellite and central body.

Our algebraic approach for the semi-major axis deviations is done through the rate of change of the satellite mechanical energy, which is equal the power applied by forces components in the transverse and radial directions. Their energy rate of change are:

$$\frac{d[E_c(t)]_r}{dt} = mv_r(t)\dot{v}_r(t), \tag{29}$$

$$\frac{d[E_c(t)]_t}{dt} = mv_t(t)\dot{v}_t(t), \tag{30}$$

$$\frac{dE_p(t)}{dt} = \frac{\mu m(t)v_r(t)}{r^2(t)}. \tag{31}$$

Adding these equations we obtain the rate of change of the satellite mechanical energy, E_M without "pitch" error,

$$\frac{dE_M(t)}{dt} = F\cos\alpha(t)v_t(t) + F\sin\alpha(t)v_r(t) \tag{32}$$

or, during the time interval Δt,

$$\Delta E_M(t_1, t_2) = E_M(t_2) - E_M(t_1)$$

$$= \int_{t_1}^{t_2} F\cos\alpha(t)v_t(t) + \sin\alpha(t)v_r(t)\,dt = \frac{-\mu m}{2a(t_2)} + \frac{\mu m}{2a(t_1)}, \tag{33}$$

with $a(t_i)$ the semi-major axis of the satellite orbit of the instant i.

Equation (33) for one transfer under "pitch" error, $\Delta\alpha(t)$ is,

$$\Delta E'_M(t_1, t_2) = E'_M(t_2) - E'_M(t_1)$$

$$= \int_{t_1}^{t_2} F(\cos[\alpha(t) + \Delta\alpha(t)]v'_t(t))\,dt + \int_{t_1}^{t_2} F(\sin[\alpha(t) + \Delta\alpha(t)]v'_r(t))\,dt. \tag{34}$$

Taking the difference between Equations (33) and (34), we obtain,

$$\Delta_2 E_M(t_1, t_2) \equiv \Delta E'_M(t_1, t_2) - \Delta E_M(t_1, t_2)$$

$$= \frac{-\mu m}{2a'(t_2)} + \frac{\mu m}{2a'(t_1)} + \frac{\mu m}{2a(t_2)} + \frac{-\mu m}{2a(t_1)}$$

$$= \int_{t_1}^{t_2} F(\cos[\alpha(t) + \Delta\alpha(t)]v'_t(t) - \cos\alpha(t)v_t(t))\,dt \tag{35}$$

$$+ \int_{t_1}^{t_2} F(\sin[\alpha(t) + \Delta\alpha(t)]v'_r(t) - \sin\alpha(t)v_r(t))\,dt.$$

If we use the fact that the semi-major axis of the initial and final orbits in the initial instant are equal, and doing some algebraic manipulation, taking the expectation ($\mathcal{E}$), of the final equation, we have,

$$\mathcal{E}[\Delta_2 E_M(t_1, t_2)] = \mathcal{E}\left[\int_{t_1}^{t_2} F\{\cos\alpha(t)[\cos\Delta\alpha(t) - 1] - \sin\alpha(t)\sin\Delta\alpha(t)\}v_t'(t)\,dt\right]$$

$$+ \mathcal{E}\left[\int_{t_1}^{t_2} F\{\sin\alpha(t)[\cos\Delta\alpha(t) - 1] + \cos\alpha(t)\sin\Delta\alpha(t)\}v_r'(t)\,dt\right] \qquad (36)$$

$$+ \mathcal{E}\left[\int_{t_1}^{t_2} F\{\cos\Delta\alpha(t)\}\{v_t'(t) - v_t(t)\}dt + F\{\sin\Delta\alpha(t)\}\{v_r'(t) - v_r(t)\}dt\right].$$

Now, we consider that the stochastic processes are ergodic. So, the expectation operator (mean in the ensemble) commutes with the integral operator (in time). Besides this, the function F and the trigonometric functions are deterministic in time. Therefore, we evaluate the mean through the ensemble for equation (36),

$$\mathcal{E}[\Delta_2 E_M(t_1, t_2)] = \int_{t_1}^{t_2} F\cos\alpha(t)\mathcal{E}[[\cos\Delta\alpha(t) - 1]v_t'(t)]\,dt$$

$$- \int_{t_1}^{t_2} F\sin\alpha(t)\mathcal{E}[\sin\Delta\alpha(t)v_t'(t)]\,dt + \int_{t_1}^{t_2} F\sin\alpha(t)\mathcal{E}[[\cos\Delta\alpha(t) - 1]v_r'(t)]\,dt$$

$$\qquad (37)$$

$$+ \int_{t_1}^{t_2} F\cos\alpha(t)\mathcal{E}[\sin\Delta\alpha(t)v_r'(t)]\,dt + \int_{t_1}^{t_2} F\cos\alpha(t)\mathcal{E}[v_t'(t) - v_t(t)]dt$$

$$+ \int_{t_1}^{t_2} F\sin\alpha(t)\mathcal{E}[v_r'(t) - v_r(t)]\,dt.$$

Equation (37) is general for any probability distribution function to $\Delta\alpha(t)$ and for any kind of noise, that is, "white-noise", "'pink-noise", or other. But, we must define if the variables inside the integral in equation (37) are correlated or not, to evaluate the expectation, as follows:

4 Case 1: $\Delta\alpha(t)$ Not Correlated with Transverse and Radial Velocities (White-Noise), Uniform Errors

In this case, we decompose the expectation operator as one product of the individual expectations for the trigonometric functions of the $\Delta\alpha(t)$ and the velocities components,

because they are not correlated. For the $\Delta\alpha(t)$ with uniform distribution inside the interval $[-\Delta\alpha_{max}, \alpha_{max}]$, we have,

$$\mathcal{E}\{[\cos\Delta\alpha(t_1) - 1]v_t'(t_1)\} = \mathcal{E}\{[\cos\Delta\alpha(t_1) - 1]\}\mathcal{E}\{v_t'(t_1)\}$$

$$= v_t(t_1)\mathcal{E}\{[\cos\Delta\alpha(t_1) - 1]\} = \{\mathcal{E}[\cos\Delta\alpha(t_1)] - \mathcal{E}(1)\}v_t(t_1)$$

$$= v_t(t_1)\frac{1}{2\Delta\alpha_{max}}\left[\int_{-\Delta\alpha_{max}}^{\Delta\alpha_{max}} d(\Delta\alpha)\cos\Delta\alpha - 1\right] \tag{38}$$

$$= \frac{1}{2\Delta\alpha_{max}}[\sin\Delta\alpha|_{-\Delta\alpha_{max}}^{\Delta\alpha_{max}} - 1]v_t(t_1) = v_t(t_1)\left[\frac{\sin\Delta\alpha_{max}}{\Delta\alpha_{max}} - 1\right]$$

and,

$$\mathcal{E}\{[\cos\Delta\alpha(t_1) - 1]v_r'(t_1)\} = v_r(t_1)\left[\frac{\sin\Delta\alpha_{max}}{\Delta\alpha_{max}} - 1\right] \tag{39}$$

with,

$$\mathcal{E}\{[\sin\Delta\alpha(t_1)]v_t'(t_1)\} = \mathcal{E}\{[\sin\Delta\alpha(t_1)]\mathcal{E}[v_t'(t_1)]\}$$

$$= v_t(t_1)\frac{1}{2\Delta\alpha_{max}}\int_{-\Delta\alpha_{max}}^{\Delta\alpha_{max}} d(\Delta\alpha)\sin\Delta\alpha \tag{40}$$

$$= v_t(t_1)\left[\frac{1}{2\Delta\alpha_{max}}\right][\cos\Delta\alpha]_{-\Delta\alpha_{max}}^{\Delta\alpha_{max}} = 0$$

and,

$$\mathcal{E}[\sin\Delta\alpha(t_1)]v_r'(t_1) = 0. \tag{41}$$

We consider that the velocities effects inside the internal $[-\Delta\alpha_{max}, \Delta\alpha_{max}]$ in the same time are, practically, balanced, because the deviations occur between values maxima and minima inside them. That is, the velocities with errors and without them are very close values. So,

$$\mathcal{E}\{v_{t,r}'(t)\} = v_{t,r}(t_1). \tag{42}$$

With these results equation (37) becomes,

$$\mathcal{E}\{\Delta_2 E_M(t_1, t_2)\} = \int_{t_1}^{t_2} F\cos\alpha(t)v_t(t)\left\{\frac{\sin\Delta\alpha_{max}}{\Delta\alpha_{max}} - 1\right\}dt$$

$$+ \int_{t_1}^{t_2} F\sin\alpha(t)v_r(t)\left\{\frac{\sin\Delta\alpha_{max}}{\Delta\alpha_{max}} - 1\right\}dt. \tag{43}$$

In other hand, we have,

$$\mathcal{E}\{\Delta_2 E_M(t_1, t_2)\} = \mathcal{E}\left\{\frac{\mu m}{2a(t_2)} - \frac{\mu m}{2a'(t_2)}\right\} = \frac{\mu m}{2}\frac{1}{a(t_2)}\mathcal{E}\left\{\frac{\Delta a(t_2)}{a'(t_2)}\right\} \tag{44}$$

with,

$$\Delta a(t_2) = a'(t_2) - a(t_2). \tag{45}$$

If we expand equation (44) about the rate $\dfrac{\Delta a(t_2)}{a(t_2)}$, we get:

$$\frac{\mu m}{2} \left[\frac{1}{a^2(t_2)} \mathcal{E}\{\Delta a(t_2)\} - \frac{1}{a^3(t_2)} \mathcal{E}\{\Delta^2 a(t_2)\} \right.$$

$$\left. + \frac{1}{a^4(t_2)} \mathcal{E}\{\Delta^3 a(t_2)\} - \frac{1}{a^5(t_2)} \mathcal{E}\{\Delta^4 a(t_2)\} + \dots \right] \tag{46}$$

$$= \frac{\mu m}{2} \sum_{n=1}^{\infty} (-1)^{n+1} \frac{1}{a^{n+1}(t_2)} \mathcal{E}\{\Delta^n a(t_2)\}.$$

We can compare equations (46) and (43), getting:

$$\sum_{n=1}^{\infty} (-1)^{n+1} \frac{1}{a^{n+1}(t_2)} \mathcal{E}\{\Delta^n a(t_2)\} = K_1 \left[\frac{\sin \Delta \alpha_{max}}{\Delta \alpha_{max}} - 1 \right]$$

$$= K_1 \left[-\frac{1}{3!} \Delta^2 \alpha_{max} + \frac{1}{5!} \Delta^4 \alpha_{max} - \frac{1}{7!} \Delta^6 \alpha_{max} + \dots \right] \tag{47}$$

$$= K_1 \sum_{n=1}^{\infty} (-1)^{n+1} \frac{1}{(2n+1)!} \Delta^{2n} \alpha_{max}$$

with,

$$K_1 = \frac{2}{\mu} \frac{(Q_1 + Q_2)}{m}, \tag{48}$$

where Q_1 and Q_2 are quadratures.

Equation (47) describes a sequence of even power terms for the maximum deviation in "pitch" with respect the expected values of the semi-major axis. For $n = 1$, we have,

$$\mathcal{E}\{\Delta a(t_2)\} = -\frac{1}{3!} \Delta^2 \alpha_{max} K_1 a^2(t_2) = -\frac{1}{3!} \Delta^2 \alpha_{max} K_2, \tag{49}$$

$$K_2 = K_1 a^2(t_2). \tag{50}$$

This result shows that in first order the cause/effect relationship is parabolic. But that the general curve would be a composition of all even power terms.

5 Case 2: $\Delta \alpha(t)$ Not Correlated with Transverse and Radial Velocities (White-Noise), Gaussian Errors

The procedures for the $\Delta \alpha(t)$ with Gaussian distribution inside the interval $[-\Delta \alpha_{max}, \Delta \alpha_{max}]$ are the same for the uniform distribution. So,

$$[\mathcal{E}\{\cos\Delta\alpha(t_1)\} - 1]v_t(t_1) = v_t(t_1)\left\{\int_{-\infty}^{\infty}\cos[\Delta\alpha]\,d(\Delta\alpha)\,\frac{e^{-\frac{(\Delta\alpha)}{2\sigma_\alpha}}}{\sqrt{2\pi}\sigma_\alpha} - 1\right\}$$

(51)

$$= v_t(t_1)\left\{e^{\frac{-\sigma_\alpha^2}{2}} - 1\right\} = v_t(t_1)\left\{-\frac{\sigma_\alpha^2}{2} + \frac{\sigma_\alpha^4}{8} - \frac{\sigma_\alpha^6}{48} + \dots\right\},$$

$$\sum_{n=1}^{\infty}(-1)^{n+1}\frac{1}{a^{n+1}(t_2)}\mathcal{E}\{\Delta^n a(t_2)\} = K_1\sum_{n=1}^{\infty}(-1)^n\frac{\sigma_\alpha^{2n}}{2^n n!}.$$

(52)

The form of the curve in equation (52) is similar that in equation (47). That is, there is a clear nonlinear relationship between cause $(\Delta\alpha_{max} = \sqrt{3}\sigma_\alpha)$ and effect $(\Delta a(t_2))$. For $n = 1$, we have,

$$\mathcal{E}\{\Delta a(t_2)\} = -\frac{1}{6}\sigma_\alpha^2 K_2.$$

(53)

6 Case 3: $\Delta\alpha(t)$ Correlated with Transverse and Radial Velocities (Pink-Noise), Uniform Errors

In this case, we cannot decompose the expectation operator as a product of the individual expectations for the trigonometric functions of the $\Delta\alpha(t)$ and the velocities components, because now they are correlated. The procedures are the same done until this point, except that we must evaluate the expectation of the products of the different variables, without decomposing them. Besides this, we consider the $\Delta\alpha(t)$ random-bias deviations, that is, $\Delta\alpha(t) = \text{constant} = \Delta\alpha(t_1) = \Delta\alpha$. After many mathematical manipulations we found the following equation, for both cases, uniform and Gaussian distribution,

$$I_{r,t} = \int_{t_2}^{t_1}\mathcal{E}\{(\cos\Delta\alpha)\ddot{v}'_{r,t}(t)\dot{f}'(t)\}\,dt.$$

(54)

We know that the integral of the odd functions for symmetrical distributions is null. But equation (54) has an even product of the functions. The odd functions inside the product are not known, but we can modeled its product as one even function, for example, $\cos\Delta\alpha$.

Other important approach in this way is to consider for equation (26) that the expectation of the product is equal the product of the expectations of the functions, so that,

$$\mathcal{E}\left\{\frac{\cos(\Delta\alpha)}{r'^2(t)}\right\} = \mathcal{E}\left\{\cos(\Delta\alpha)\frac{1}{r'^2(t)}\right\} \cong \mathcal{E}\{\cos(\Delta\alpha)\}\mathcal{E}\left\{\frac{1}{r'^2(t)}\right\} = \frac{\mathcal{E}\{\cos(\Delta\alpha)\}}{r^2(t)}.$$

(55)

The final forms are:

$$\sum_{n=1}^{\infty}(-1)^{n+1}\frac{1}{a^{n+1}(t_2)}\mathcal{E}\{\Delta^n a(t_2)\} = \lambda_1 - \lambda_2\Delta^2\alpha_{max} + \lambda_3\Delta^4\alpha_{max} - \dots$$

(56)

for the uniform case and,

$$\sum_{n=1}^{\infty}(-1)^{n+1}\frac{1}{a^{n+1}(t_2)}\mathcal{E}\{\Delta^n a(t_2)\} = \lambda_4 - \lambda_5\sigma_\alpha^2 + \lambda_6\sigma_\alpha^4 - \lambda_7\sigma_\alpha^6 + \dots \qquad (57)$$

for the Gaussian case, where the coefficients are

$$\lambda_1 = Q_8[Q_5 + Q_6 - v_t(t_1)] + Q_{12}[Q_{10} + Q_3 - v_r(t_1)], \qquad (58)$$

$$\lambda_2 = \left\{[2Q_3Q_{12} - Q_8Q_4 + Q_8Q_5]\left[\frac{1}{2}\frac{1}{2!} + \frac{1}{2}\frac{1}{3!}\right] + [Q_{10}Q_{12} + Q_8Q_6 + Q_8Q_5]\frac{1}{3!}\right\}, (59)$$

$$\lambda_3 = \left\{[-Q_8Q_4 + Q_8Q_5]\left[\frac{1}{2}\frac{1}{2!}\frac{1}{3!} + \frac{1}{2}\frac{1}{4!}\right] + \frac{1}{3!}[Q_6 + Q_{10}Q_{12}] + \frac{Q_8Q_5}{7!} - \frac{Q_{12}Q_3}{2}\frac{1}{5!}\right\}, (60)$$

$$\lambda_4 = Q_8[Q_6 - v_t(t_1)] + Q_{12}[Q_{11} - v_r(t_1)], \qquad (61)$$

$$\lambda_5 = Q_{12} + \frac{Q_8Q_6}{2} - Q_8Q_4 + Q_{12}Q_{11,1}, \qquad (62)$$

$$\lambda_6 = Q_{12} + \frac{Q_8Q_6}{8} - Q_8Q_4 + Q_{12}Q_{11,2}, \qquad (63)$$

$$\lambda_7 = \frac{2}{3}Q_{12} + \frac{Q_8Q_6}{48} - \frac{2}{3}Q_8Q_4 + Q_{12}Q_{11,3}. \qquad (64)$$

The Q_{ij} functions are quadratures. The first order for both cases are:

$$\mathcal{E}\{\Delta a(t_2)\} = \lambda_1 a^2(t_2) - \lambda_2 a^2(t_2)\Delta^2\alpha_{max} \qquad (65)$$

for the uniform case and,

$$\mathcal{E}\{\Delta a(t_2)\} = \lambda_4 a^2(t_2) - \lambda_5 a^2(t_2)\sigma_\alpha^2, \qquad (66)$$

for the Gaussian case.

These results show once more the nonlinear relationship between cause and effect. The terms $\lambda_1 a^2(t_2)$ and $\lambda_4 a^2(t_2)$ are constants and do not change the general form of the curves. We can compare both results of the deviations (uniform and Gaussian) by relating,

$$\Delta\alpha_{max} = \sqrt{3}\sigma_\alpha. \qquad (67)$$

If we replace this equation inside equation (47), we conclude that:

(a) for the first order the results are the same, for the same σ_α;

(b) for other orders, the Gaussian semi-major axis deviations are $\dfrac{(2n+1)!}{6^n n!}$ greater than the uniform deviations, for the same σ_α.

7 Transfers with Errors in the Thrust Vector: Numerical Analysis

The numerical results confirm the algebraic results obtained. We simulated (Monte-Carlo) 1000 ensembles of the transfer trajectories for both kind of deviations (uniform-U, Gaussian-G), for both maneuvers ("theoretical"-T, "practical"-P), for random bias (S) and white noise (O) deviations. Figures 7.1 and 7.2 show $\mathcal{E}[a(t_2)]$ for cases TUS, TUO, TGS, TGO, and PUS, PUO, PGS, PGO, respectively.
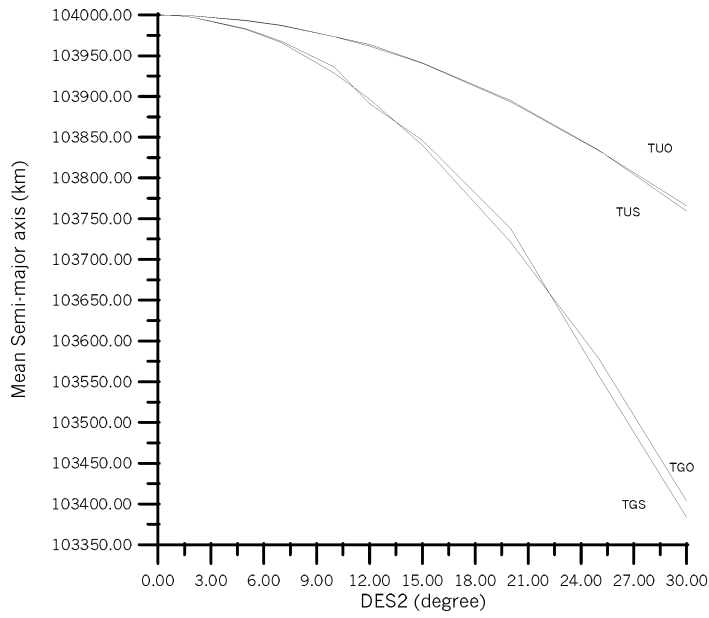
Figure 7.1.   Mean semi-major axis × DES2, Theoretical Orbits.

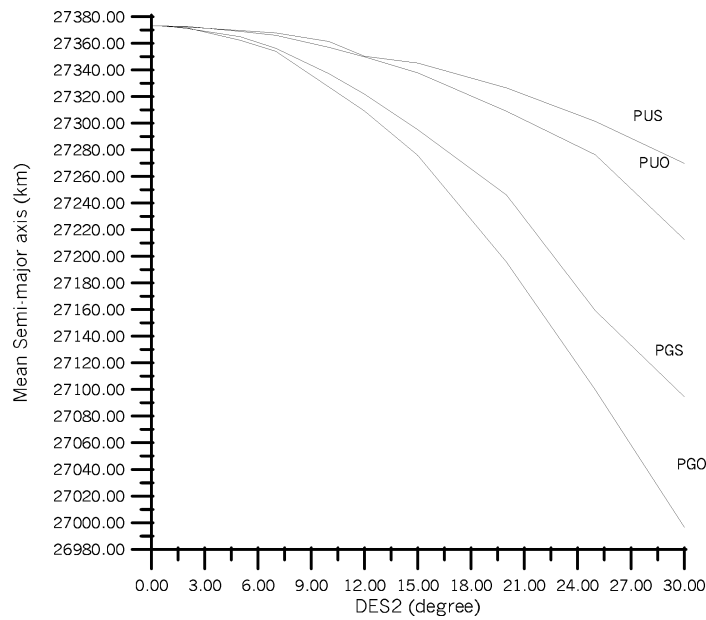**Figure 7.2**.   Mean semi-major axis × DES2, Practical Orbits.

In these figures $DES2 = \sqrt{3}\sigma_{\Delta\alpha}$, where $\sigma_{\Delta\alpha}$ is the pitch angle standard deviation for zero mean. We can observe clearly the nonlinear shapes of the curves like parabolas. The numerical results for the relation between uniform and Gaussian deviations confirms equation (67). Figures 7.3, 7.4, 7.5 and 7.6 show that the Gaussian deviations (ΔG) are more than the uniform deviations (ΔU).
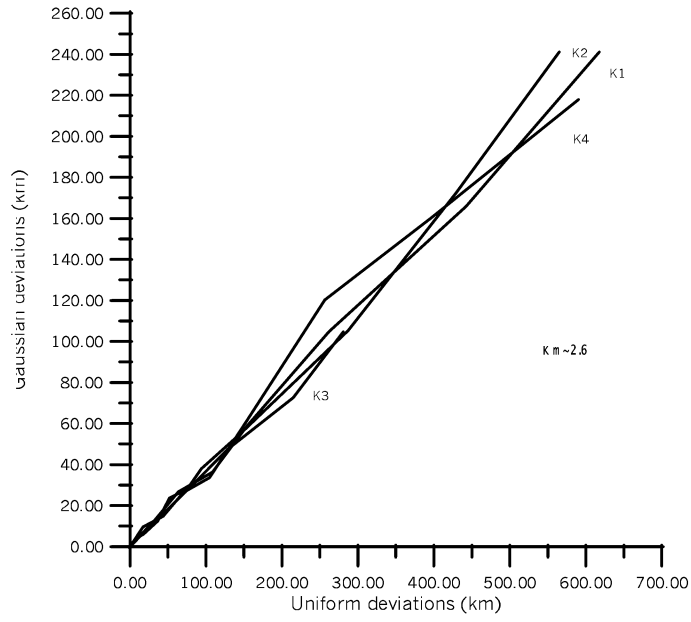
Figure 7.3. $\Delta G \times \Delta U$: Theoretical and Practical Cases, Systematic Errors.
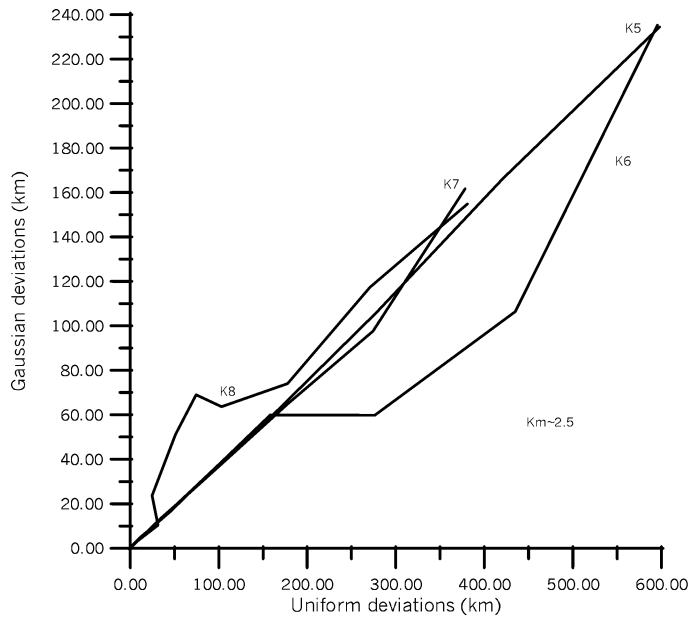

Figure 7.4. $\Delta G \times \Delta U$: Theoretical and Practical Cases, Operational Errors.
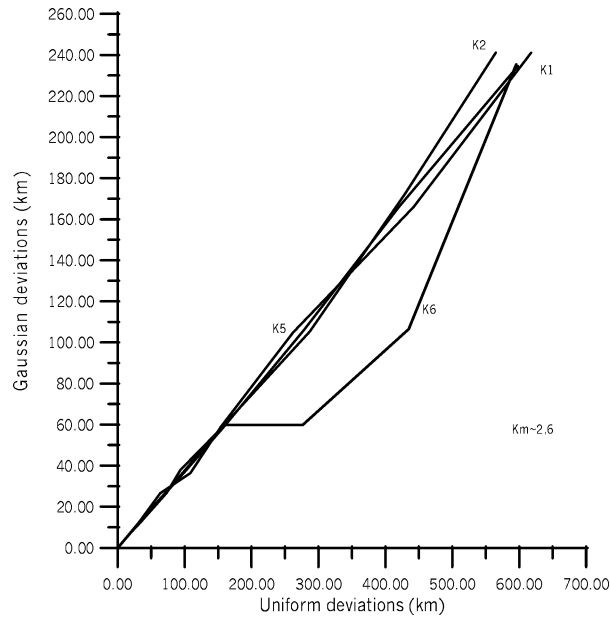
Figure 7.5. $\Delta G \times \Delta U$: Theoretical Case, Systematic and Operational Errors.
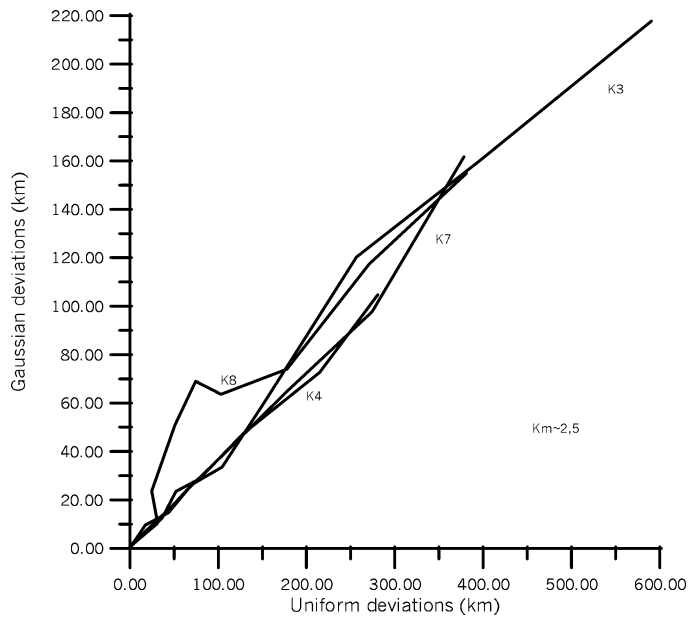

Figure 7.6. $\Delta G \times \Delta U$: Practical Case, Systematic and Operational Errors.

The mean linear coefficient between them is 2.6 in all cases: TUS, TUO, TGS, TGO and PUS, PUO, PGS, PGO. In theses graphics we introduced the numerical results of the out-plane angle deviations, that is, "yaw" angle deviations, DES3. The linear coefficients for these angle deviation are: k_2, k_4, k_6 and k_8, while for the "pitch" angle deviation,

k_1, k_3, k_5 and k_7. The algebraic results in equation (67) anticipated the value 3 (≈ 2.6 for numerical results). This shows consistency of our results.

8 Conclusions

In the algebraic developments, we obtained expression for $\mathcal{E}\{\Delta a(t_2)\}$ as series of even powers of $\sigma_{\Delta\alpha}$ dominated by the $(\sigma_{\Delta\alpha})^2$ term, to explain the near parabolic relations and others found, independent of the: 1) transfer orbit ("theoretical" or "practical"); 2) ensemble distribution (uniform or Gaussian); 3) time correlation/dependence (random-bias or white-noise). These results suggest and partially characterizes the progressive deformation of the trajectory distribution along the propulsive arc, turning 3-sigma ellipsoids into "banana" shaped volumes curved to the center of attraction (we call them "bananoids") due to the loss of optimality of the actual (with errors) trajectories with respect to the nominal (no errors) trajectory. A similar deformation but due to: a) the mean drag was studied by Carlton-Wippern [15]; b) initial condition Gaussian errors was shown by Junkins [14]. As his plots also suggest, such deformations can not be anticipated by covariance analysis ([9, 10, 12]) on linearized models with zero mean errors which propagate ellipsoids into ellipsoids always centered in the nominal (no errors) trajectory. Those results also characterize how close/far are Monte-Carlo analysis and covariance analysis for those examples. Other details about our numerical results can be found in Jesus [23].

References

[1] Marec, J.P. *Optimal Space Trajectories*. Elsevier, New York, 1979.

[2] Jesus, A.D.C. Análise estatística de manobras orbitais com propulsão finita sujeita a erros no vetor empuxo. *Doctoral Thesis*. Instituto Nacional de Pesquisas Espaciais (INPE), São José dos Campos, São Paulo, Brasil, 1999.

[3] Schwende, M.A. and Strobl, H. Bi-propellant propulsion systems for spacecraft injection and control. *Attitude and Orbit Control Systems. Proceedings, ESA, Paris*, 1997, pp. 405–412.

[4] Tandon, G.K. Modeling torques due to orbit maneuvers. *Astrophysics and Space Science Library* **733** (1988) 580–583.

[5] Rodrigues, D.L.F. Análise dinâmica da transferência orbital. *Master Dissertation*. Instituto Nacional de Pesquisas Espaciais (INPE), São José dos Campos, São Paulo, Brasil, 1991. (INPE-5352-TDI/461).

[6] Santos-Paulo, M.M.N. Estudo de manobras tridimensionais impulsivas pelo método de Altman e Pistiner, com erros nos propulsores. *Master Dissertation*. Instituto Nacional de Pesquisas Espaciais (INPE). São José dos Campos, São Paulo, Brasil, 1998.

[7] Rocco, E.M. Transferências orbitais bi-impulsivas com limite de tempo e erros no vetor empuxo. *Doctoral Thesis (on going)*. Instituto Nacional de Pesquisas Espaciais (INPE), São José dos Campos, São Paulo, Brasil, 1999.

[8] Schultz, W. Transferências biimpulsivas entre órbitas elípticas não coplanares com consumo mínimo de combustível. Master Dissertation. Instituto Nacional de Pesquisas Espaciais (INPE), São José dos Campos, São Paulo, Brasil, 1997.

[9] Porcelli, G. and Vogel, E. Two-impulse orbit transfer error analysis via covariance matrix. *Journal of Spacecraft and Rockets* **17**(3) (1980) 285–255.

[10] Adams, N.J. and Melton, R.G. Orbit transfer error analysis for multiple, finite perigee burn, ascent trajectories. *The Journal of Astronautical Sciences* **34**(4) (1986) 355–373.

[11] Rao, K.R. Orbit error estimation in the presence of force model errors. *AAS Paper 93-254, Advances in the Astronautical Sciences* **84**(1) (1993) 61–74.

[12] Howell, K.C. and Gordon, S.C. Orbit determination error analysis and a station-keeping strategy for Sun-5-Earth L1 libration point orbits. *The Journal of Astronautical Sciences* **42**(2) (1994) 207–228.

[13] Junkins, J.L., Akella, M.R. and Alfried, K.T. Non-gaussian error propagation in orbit mechanics. *The Journal of the Astronautical Sciences* **4**(4) (1996) 541–563.

[14] Junkins, J.L. Adventures on the interface of dynamics and control. *Journal of Guidance, Control, and Dynamics* **20**(6) (1997) 1058–1071.

[15] Carlton-Wippern, K.C. Satellite position dilution of precision (SPDOP). *AAS/AIAA Astrodynamics Specialist Conference*, Sun Valley, Idaho, EUA, August 4-7, 1997, (AAS 97-609).

[16] Alfriend, K.T. Orbit uncertainty due to drag uncertainty. 14th *International Symposium on Spaceflight Systems and Data Control*, Iguassu Falls, Parana, Brazil, February 8-12, 1999.

[17] Jesus, A.D.C., Souza, M.L.O. and Prado, A.F.B. Monte-Carlo analysis of nonimpulsive orbital transfer under thrust errors, 1. *Advances in the Astronautical Sciences*, USA, **103**(3) (2000) 1923–1936. *AAS/AIAA Astrodynamics Specialist Conference*, Girdwood, Alaska, USA, August 16-19 (Paper AAS 99-424).

[18] Jesus, A.D.C., Souza, M.L.O. and Prado, A.F.B. Monte-Carlo analysis of nonimpulsive orbital transfer under thrust errors, 2. *Nonlinear Dynamics, Chaos, Control and Their Applications to Engineering Sciences* **4**: *Recent Developments in Nonlinear Phenomena*. Rio Claro **4** (2000) 379–389.

[19] Biggs, M.C.B. The Optimisation of Spacecraft Orbital Manoeuvres. Part I: Linearly Varying Thrust Angles. Connecticut, USA: The Hatfield Polytechnic, Numerical Optimisation Centre, 1978. 24p. (The Hatfield Polytechnic – Technical Report 98).

[20] Biggs, M.C.B. The optimisation of spacecraft orbital manoeuvres. Part II: Using Pontryagin's Maximum Principle. Connecticut, USA: The Hatfield Polytechnic, Numerical Optimisation Centre, 1979. 27p. (The Hatfield Polytechnic – Technical Report 101).

[21] Prado, A.F.B.A. Análise, seleção e implementação de procedimentos que visem manobras ótimas de satélites artificiais. Master Dissertation. Instituto Nacional de Pesquisas Espaciais (INPE), São José dos Campos, São Paulo, Brasil, 1989. (INPE-5003-TDL/397).

[22] Kuga, H.K., Gill, E. and Montenbruck, O. Orbit determination and apogee boost maneuver estimation using UD filtering. Wessling: DLR-GSOC, 1991. (Internal report DLR-GSOC IB 91-2).

[23] Jesus, A.D.C., Souza, M.L.O. and Prado, A.F.B. Statistical analysis of nonimpulsive orbital transfers under thruster errors, 1. *Nonlinear Dynamics and Systems Theory* **2**(2) (2002) 157–172.